

Pointly-supervised 3D Scene Parsing with Viewpoint Bottleneck

Liyi Luo^{1,2}, Beiwen Tian¹, Hao Zhao³ and Guyue Zhou¹

Abstract—Semantic understanding of 3D point clouds is important for various robotics applications. Given that point-wise semantic annotation is expensive, in this paper, we address the challenge of learning models with *extremely sparse labels*. The core problem is how to leverage numerous unlabeled points. To this end, we propose a self-supervised 3D representation learning framework named *viewpoint bottleneck*. It optimizes a mutual-information based objective, which is applied on point clouds under different viewpoints. A principled analysis shows that viewpoint bottleneck leads to an elegant surrogate loss function that is suitable for large-scale point cloud data. Compared with former arts based upon contrastive learning, viewpoint bottleneck operates on the feature dimension instead of the sample dimension. This paradigm shift has several advantages: It is easy to implement and tune, does not need negative samples and performs better on our goal down-streaming task. We evaluate our method on the public benchmark ScanNet, under the pointly-supervised setting. We achieve the best quantitative results among comparable solutions. Meanwhile we provide an extensive qualitative inspection on various challenging scenes. They demonstrate that our models can produce fairly good scene parsing results for robotics applications. Our code, data and models will be made public.

I. INTRODUCTION

We study the problem of dense semantic parsing of 3D point clouds. As illustrated by Fig. 1-(a), a bedroom can be reconstructed by TSDF-based fusion methods like [1] [2]. Then taking it as input, a 3D scene parsing network generates a semantic label for each point in it, as demonstrated by Fig. 1-(f). This is a core environment sensing capability for intelligent robots. Knowing the semantic class of the 3D world lays the foundation for decision making. However, training such a model needs point-wise annotation, which is very expensive and time-consuming to obtain. As such, we address the challenge of learning such models using an extremely small subset of annotations. For example, Fig. 1-(e) shows the parsing result generated by a model trained using 200 points per scene, which is almost as good as Fig. 1-(f). Since a scene in the ScanNet database [3] typically contains more than 50000 points, a subset of 200 points only amounts to 0.4% data usage.

The key to effective pointly-supervised learning is leveraging numerous unlabelled points (e.g., the other 99.6% data in the aforementioned case). If we can learn meaningful representations from them without the usage of semantic annotation, a subsequent pointly-supervised fine-tuning is expected to give good results. This is usually referred to

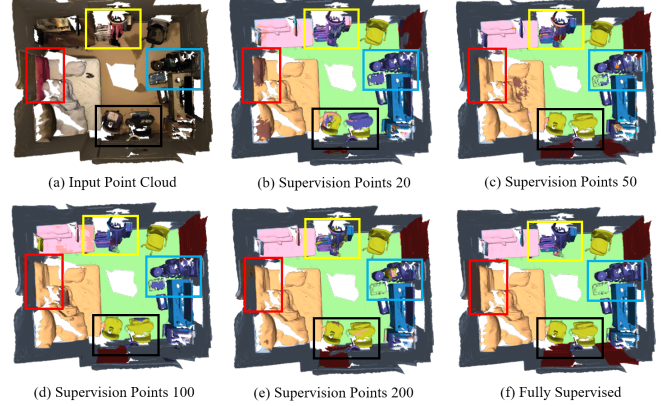


Fig. 1. We address the challenging problem of learning 3D scene parsing models using only semantic annotations on limited points (20 to 200 points per scene). (a) shows a point cloud of an indoor scene. (b)-(e) demonstrate 3D semantic understanding results using 20 to 200 point annotations per scene. (f) shows the result generated by a fully supervised model. Except for highlighted regions in boxes, most points are correctly segmented, showing the effectiveness of our viewpoint bottleneck method.

as self-supervised representation learning (SSRL). While exciting progress has been achieved in 2D SSRL [4] [5] [6], 3D SSRL in point clouds [7] [8] is still an under-explored emerging topic. Many open problems exist and challenge the effectiveness of existing 3D SSRL methods:

(1) Former 2D SSRL methods treat each image as a sample. While 3D SSRL for dense semantic parsing naturally requires us to treat each point as a sample. This fact leads to an extremely large sample set.

(2) Former contrastive learning methods operate on the sample dimension. As conceptually shown in Fig. 2-left, embeddings for the same sample under different viewpoints are drawn near, and embeddings for different samples are pushed away. Selecting good sample pairs is an unclear and difficult problem, especially when the 3D sample set is large.

(3) Former contrastive learning methods are troubled with degenerated solutions thus requires sophisticated techniques to break the symmetry like weight averaging with momentum [6]. Complex implementation details make them hard to tune.

Very recently, several works [10] [11] [12] propose to switch representation learning from the sample dimension to the feature dimension. Inspired by them, we propose a new 3D representation learning method called *viewpoint bottleneck*. It starts with an objective defined with the mutual information between features and samples. A principled analysis under mild distribution assumptions shows that an efficient surrogate loss implementation can be used to optimize the objective. The surrogate loss is conceptually shown

¹ Institute for AI Industry Research (AIR), Tsinghua University, China tbw18@mails.tsinghua.edu.cn, zhouguyue@air.tsinghua.edu.cn

² McGill University, Canada liyi.luo@mail.mcgill.ca

³ Intel Labs China, Peking University, China zhao-hao@pku.edu.cn, hao.zhao@intel.com

in Fig. 2-right. In one word, it maximizes the correlation between corresponding feature channels while decorrelates different feature channels. This paradigm shift brings some advantages over former 3D SSRL methods based on contrastive learning, like PointContrast [7] or Contrastive Scene Context [8]. There is no need to select sample pairs or design sophisticated symmetry breaking techniques, leading to a simple implementation. This simpleness does not come with a prize of performance drop. By contrast, viewpoint bottleneck is more effective than the state-of-the-art (SOTA) method Contrastive Scene Context [8]. When evaluated on our goal downstream task pointly-supervised scene parsing, it consistently out-performs [8] in all inspected settings. To summarize, we make following contributions:

- We propose a new self-supervised 3D representation learning framework named viewpoint bottleneck, which is free of typical drawbacks of contrastive learning.
- We provide a principled analysis to motivate viewpoint bottleneck, which is absent in former 3D SSRL methods based upon contrastive learning.
- We demonstrate the effectiveness of learned representations for pointly-supervised scene parsing. We evaluate on the public benchmark ScanNet and achieve consistently better results than existing SOTA 3D SSRL solutions. A public implementation is provided.

II. RELATED WORK

A. Self-supervised Representation Learning

SSRL is a special form of unsupervised learning, which aims to learn meaningful representations of the input data without relying on annotations. The common ground of these methods is to learn representations that are invariant to distortions. There are several different ways to achieve this generic principle. For example, early attempts use different surrogate tasks whose labels can be naturally generated, like pixel value inpainting [21] [23], cross-channel feature regression [22], or rotation prediction [24]. Recently, contrastive learning [27], which was firstly proposed for metric learning, has drawn significant attention and witnessed great success for SSRL. However, it is now clear that a trivial contrastive learning formulation suffers from degeneration. As such, many variants have been proposed to address the issue like weight averaging [6] [28] or stop gradient [29] among others [14] [26].

Compared to its 2D counterpart, 3D SSRL is more urgent because of the difficulty of annotating 3D data. There are already some pioneering works that address the 3D SSRL problem borrowing ideas of contrastive learning, like PointContrast [7] and Contrastive Scene Contexts [8]. The former proposes a PointInfoNCE loss and verifies its effectiveness on a diverse set of scene understanding tasks. However, it ignores the spatial context around local points, which limits its transferability to complex downstream tasks. The latter introduces a loss function that contrasts features aggregated in local partitions. It demonstrates the possibility of using extremely few annotations to obtain good performance on a

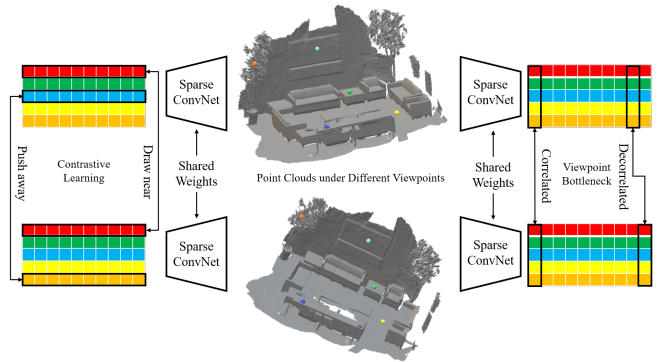


Fig. 2. Five colored dots demonstrate five point samples, under random geometric transformations. Vectors of corresponding colors demonstrate features generated by a shared Sparse ConvNet. Conventional contrastive learning methods are shown in the left. Same samples under different viewpoints (red) are drawn near while different samples (blue and orange) are pushed away, in the embedding space. Viewpoint bottleneck is shown in the right. It operates on the feature dimension instead of the sample dimension. The corresponding channel is correlated while different channels are decorrelated.

series of weakly-supervised settings. [9] [13] propose to use multi-modal pairs and tuples as elements for RGB-D contrastive learning and scene understanding. [35] develops a sophisticated spatio-temporal contrastive learning framework for point clouds.

To address the common issues of contrastive learning, a recent SSRL method [10] proposes an objective function that measures the cross-correlation matrix between the representations of two distorted versions of a sample. It naturally avoids representation collapse and sample selection since no negative samples are required. [11] [12] enrich this new scheme with a variance term and a principled kernel-based statistical measure. Inspired by them, we propose the viewpoint bottleneck principle, which is the first non-contrastive 3D SSRL method.

B. Weakly-supervised Scene Parsing

State-of-the-art scene parsing approaches generally depend on expensive sample-wise annotation to obtain good performance. To this end, many weakly-supervised solutions are proposed. [15] exploits deep metric learning to regularize the embedding, while collecting pseudo labels online by expansion. [25] identifies a statistical phenomenon called uncertainty mixture to harvest labels in an unsupervised manner. BoxSup [16] generates pseudo labels by evaluating the overlap between box supervision and bottom-up region proposals. STC [17] treats salient regions as the initial pseudo labels for image-level semantic classes. [18] proposes a method that exploits class activation maps (CAMs) to generate positive and negative affinity labels for pixel pairs. For 3D parsing, [19] generates pseudo point-wise labels by applying CAM on sub-point-clouds. [20] transfers 2D image annotations to 3D space to produce labels in point cloud. In this paper, we follow the path of 3D SSRL introduced by [7] [8] and propose a formulation free of sample selection.

III. METHOD

In this section, we describe the procedure of learning pointily-supervised scene parsing models with viewpoint bottleneck. As shown in Fig.3, our approach is consisted of two stages: (1) a 3D SSRL stage using the newly proposed viewpoint bottleneck loss, and (2) fine-tuning the pretrained model for scene parsing with point supervision.

A. Overview

A fully-supervised 3D scene parsing dataset is denoted as $\{P_i, L_i\}, i \in \{1, 2, \dots, N\}$, in which $P_i (M \times 6)$ is the point cloud represented by the concatenation of 3D coordinates and colors and $L_i (M \times 1)$ is the point-wise semantic label set for P_i . A weakly-supervised 3D scene parsing dataset is depicted as $\{P_i, S_i\}$, where S_i is an annotation-efficient version of L_i . In S_i , only few points have been labeled and other points' labels are set to *None*. Firstly, we train a pre-trained model $VB(*, \Theta)$ only using P_i , as shown in Fig.3-(A). Secondly, we fine-tune the pre-trained model $VB(*, \Theta)$ with the weakly-supervised scene parsing dataset $\{P_i, S_i\}$. A new prediction head is added as illustrated by the light blue block in Fig.3-(B). The network parameterized by Ψ predicts the probability $Q(y_{ijs}|P_{ij}; \Psi)$, in which j indexes points in P_i and s indexes semantic categories. We train it with the Softmax cross-entropy loss as below:

$$L_{ce} = -\frac{1}{NM} \sum_{i=1}^N \sum_{j=1}^M -\log Q(y_{ijs}|\bar{s}; P_{ij}; \Psi) \quad (1)$$

Note here \bar{s} is the ground truth label for P_{ij} . Finally, we run the trained scene parsing model, as in Fig.3-(C).

B. Self-supervised Pre-training

Here we describe our self-supervised learning stage.

Firstly, a point cloud $X = \{p_i\}$ is augmented into two viewpoints by random geometric transformations. Transformed 3D point clouds are denoted by $X_p = \{p'_i\}$ and $X_q = \{p''_i\}$ respectively. As Fig. 4 shows, these two randomly transformed point clouds are fed into the same sparse convolutional network f_θ to obtain two high-dimensional representations $Z_p = f_\theta(X_p)$ and $Z_q = f_\theta(X_q)$.

Next, we sample the representations by Farthest Point Sampling (FPS) from $M \times D$ to $H \times D$, where D is the dimension of the representations and M, H are the numbers of points before and after sampling. FPS starts with a random point as the first proposal candidate, and iteratively selects the farthest point from the already selected points until H candidates are selected. We set $H \ll M$ to keep computation tractable, while FPS guarantees that the sampled subset is a reasonable abstraction of the original point cloud.

After FPS, the cross-correlation matrix $\mathcal{Z} (D \times D)$ is computed on the batch dimension, from two sampled representations Z'_p and Z'_q . Finally, the network is trained with the proposed viewpoint bottleneck loss as detailed later.

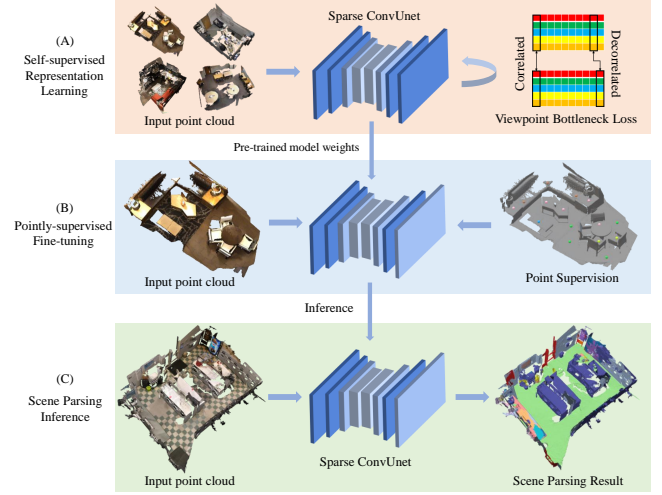


Fig. 3. The overall pipeline of our method. In the first stage (A), we pretrain the backbone network with a self-supervised learning objective named viewpoint bottleneck. In the second stage (B), we fine-tune the weights from (A) for scene parsing, while only using a very small number of annotated points. Finally, we illustrate an inference stage (C).

C. Viewpoint Bottleneck: Analysis

Inspired by Barlow Twins [10], we derive our viewpoint bottleneck objective from an information theory perspective [30] [31]. As shown in Fig.5, the information bottleneck principle assumes that meaningful representations should reserve as much information as possible about the input, while affected by random viewpoint transformations as little as possible. Formally the objective is stated as:

$$VB_\theta \triangleq I(C_\theta, B) - \beta I(C_\theta, A) \quad (2)$$

where $I(\cdot, \cdot)$ is mutual information between two random vectors. Here A, B , and C_θ correspond to input point clouds, randomly transformed point clouds and learnt representations respectively. β is a balancing weight. By definition, the mutual information can be calculated as $I(C_\theta, B) = H(C_\theta) - H(C_\theta|B)$ (similarly for $I(C_\theta, A)$). $H(C_\theta)$ is the entropy of C_θ while $H(C_\theta|B)$ is the conditional entropy of C_θ given B . As the function f_θ is deterministic, $H(C_\theta|B)$ cancels to 0. We rewrite the Eq.2 as:

$$VB_\theta = H(C_\theta) - \beta [H(C_\theta) - H(C_\theta|A)] \quad (3)$$

By dividing Eq.3 with β , we have:

$$VB_\theta = H(C_\theta|A) + \frac{1-\beta}{\beta} H(C_\theta) \quad (4)$$

However, the optimization of VB_θ becomes a challenge as evaluating the entropy of a generic random vector is intractable. We derive a surrogate loss as below:

We assume the representation C_θ is distributed as a Gaussian: $C_\theta = (c_{\theta i})_{i=1}^D \sim \mathcal{N}_D(\mu, \Sigma_{C_\theta})$. Σ_{C_θ} can be decomposed into $\Sigma_{C_\theta} = E^T E$, and $Y = E^{-1}(\tilde{C}_\theta - \tilde{\mu}) \sim \mathcal{N}(\tilde{0}, I)$. In the following derivation, $|\cdot|$ means taking determinant. The

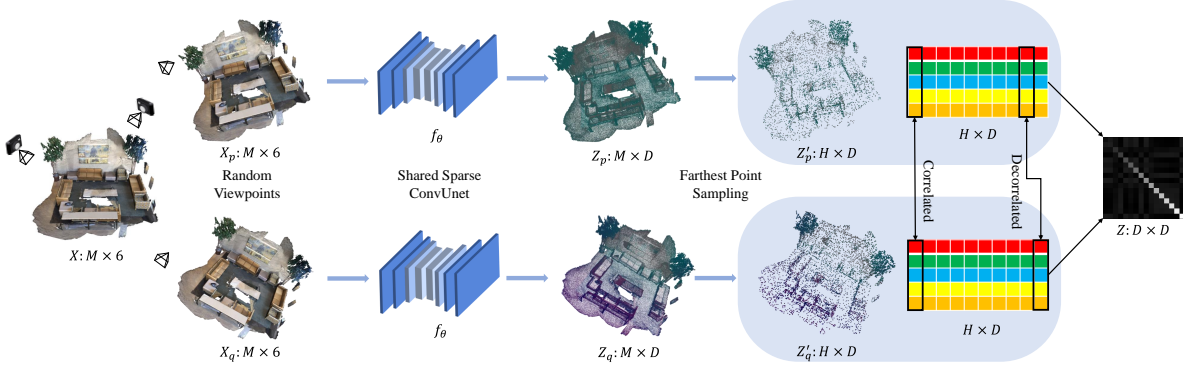


Fig. 4. Illustration of viewpoint bottleneck. X is a point cloud represented by the concatenation of 3D coordinates and colors. After two random geometric transformations, we obtain its two augmentations X_p and X_q . They are sent to a shared Sparse ConvNet f_θ , forming two high-dimensional feature sets Z_p and Z_q . To keep computation tractable, we apply farthest point sampling on them to get down-sampled Z'_p and Z'_q . Finally, the viewpoint bottleneck is imposed on the cross-correlation matrix between Z'_p and Z'_q , which is denoted as Z .

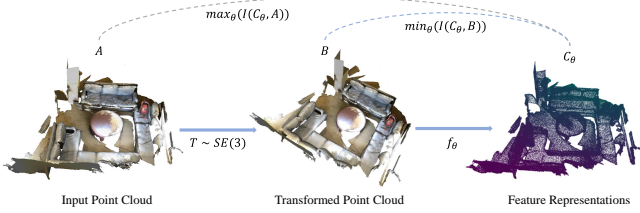


Fig. 5. A conceptual illustration of the viewpoint bottleneck principle, in which A , B and C_θ are random vectors, representing the original input point clouds, randomly transformed point clouds and high-dimensional representations generated by f_θ respectively. We aim to minimize the mutual information between B and C_θ and maximize the mutual information between A and C_θ . As such, there exists a bottleneck at B .

probability density function of C_θ is:

$$p(c_{\theta 1}, c_{\theta 2}, \dots, c_{\theta D}) = \frac{1}{(2\pi)^{\frac{D}{2}} |\Sigma_{C_\theta}|^{\frac{1}{2}}} e^{-\frac{1}{2} [(\vec{C}_\theta - \vec{\mu})^T \Sigma_{C_\theta}^{-1} (\vec{C}_\theta - \vec{\mu})]} \quad (5)$$

Then according to [33]:

$$\begin{aligned} H(C_\theta) &= - \int p(c_\theta) \log p(c_\theta) dc_\theta \\ &= - \int p(c_\theta) \log \frac{e^{-\frac{1}{2} (\vec{C}_\theta - \vec{\mu})^T \Sigma_{C_\theta}^{-1} (\vec{C}_\theta - \vec{\mu})}}{(2\pi)^{\frac{D}{2}} |\Sigma_{C_\theta}|^{\frac{1}{2}}} dc_\theta \\ &= - \int p(c_\theta) \log \frac{1}{(2\pi)^{\frac{D}{2}} |\Sigma_{C_\theta}|^{\frac{1}{2}}} dc_\theta \\ &\quad - \int p(c_\theta) \log e^{-\frac{1}{2} (\vec{C}_\theta - \vec{\mu})^T (E^{-1})^T E^{-1} (\vec{C}_\theta - \vec{\mu})} dc_\theta \\ &= \log(2\pi)^{\frac{D}{2}} |\Sigma_{C_\theta}|^{\frac{1}{2}} - \int p(Y) \log e^{-\frac{1}{2} Y^T Y} dY \\ &= \log(2\pi)^{\frac{D}{2}} |\Sigma_{C_\theta}|^{\frac{1}{2}} - \sum_{i=1}^D \log e^{-\frac{1}{2} |y_i|^2} \\ &= \log(2\pi)^{\frac{D}{2}} |\Sigma_{C_\theta}|^{\frac{1}{2}} + \log e^{\frac{D}{2}} \\ &= \frac{1}{2} \log(2\pi e)^D |\Sigma_{C_\theta}| \end{aligned} \quad (6)$$

Algorithm 1: 3D SSRL with Viewpoint Bottleneck

Input:

- 1 \mathbb{X} : a set of 3D point clouds;
- 2 \mathcal{T} : the distribution of geometric transformations;
- 3 f_θ : sparse ConvNet parameterized by θ ;
- 4 K : the number of optimization steps;
- 5 λ : the control parameter in VB loss

Output: feature network f_θ

```

1 for  $k = 1$  to  $K$  do
    /* sample transformations */
2    $T_p, T_q \sim \mathcal{T}$ 
    /* take an input point cloud */
3    $X \in \mathbb{X}$ 
    /* apply transformations */
4    $X_p = T_p(X), X_q = T_q(X)$ 
    /* extract features */
5    $Z_p = f_{\theta_k}(X_p), Z_q = f_{\theta_k}(X_q)$ 
    /* farthest point sampling */
6    $Z'_p = \text{FPS}(Z_p), Z'_q = \text{FPS}(Z_q)$ 
    /* calculate cross-correlation */
7    $\mathcal{Z} = (Z'_p)^T Z'_q$ 
    /* calculate VB loss */
8    $\mathcal{L}_{\text{VB}} = \|\Gamma_\lambda(\mathcal{Z}) - \mathcal{I}\|_F$ 
    /* optimize network parameters */
9    $\theta_{k+1} = \text{optim}(\theta_k, \mathcal{L}_{\text{VB}})$ 
10 end
```

$$\begin{aligned} H(C_\theta|A) &= \sum_a p(a) H(C_\theta|A=a) \\ &= \frac{1}{2} \mathbb{E}_A \log(2\pi e)^n |\Sigma_{C_\theta|A}| \end{aligned} \quad (7)$$

As such the viewpoint bottleneck objective Eq.4 is turned into a practical surrogate loss function as:

$$\text{VB}_\theta = \mathbb{E}_A \log |\Sigma_{C_\theta|A}| + \frac{1-\beta}{\beta} \log |\Sigma_{C_\theta}| \quad (8)$$

TABLE I
POINTLY-SUPERVISED 3D PARSING RESULTS ON THE SCANNET
VALIDATION SET (MIOU:%)

Points	200	100	50	20
Baseline	64.3	60.6	55.4	45.9
CSC [8]	68.2 (+3.9)	65.9 (+5.3)	60.5 (+5.1)	55.5 (+9.6)
VB (256)	68.4 (+4.1)	66.5 (+5.9)	63.3 (+7.9)	56.2(+10.3)
VB (512)	68.5 (+4.2)	66.8 (+6.2)	63.6 (+8.2)	57.0 (+11.1)
VB (1024)	68.4 (+4.1)	66.5 (+5.9)	63.7 (+8.3)	56.3 (+10.4)

TABLE II
RESULTS REPORTED BY SCANNET ONLINE TEST SERVER (MIOU:%)

Points	200	100	50	20
Viewpoint.BN.LA.AIR (ours)	66.9	65.0	62.3	54.8
CSC.LA.SEM [8]	66.5	64.4	61.2	53.1
PointContrast.LA.SEM [7]	65.3	63.6	61.4	55.0

Finally, we make several more simplifications: 1) Since Eq.8 is only meaningful when $\beta > 1$, we use a positive constant λ to replace $\frac{\beta-1}{\beta}$. 2) In the second term of the Eq.8 we use the Frobenius norm of Σ_{C_θ} as the metric. 3) Recall that the first term of Eq.8 is derived from the conditional entropy of the representation C_θ given A . Minimizing it is equivalent to maximizing the diagonal elements of \mathcal{Z} (the aforementioned $D \times D$ cross-correlation matrix).

D. Viewpoint Bottleneck: Implementation

After making aforementioned three simplifications to Eq.8, we obtain the final viewpoint bottleneck loss function as:

$$\mathcal{L}_{VB} \triangleq \|\Gamma_\lambda(\mathcal{Z}) - \mathcal{I}\|_F \quad (9)$$

where \mathcal{I} denotes the identity matrix, $\Gamma_\lambda(\cdot)$ denotes scaling off-diagonal elements by positive constant λ , and \mathcal{Z} is the cross-correlation matrix computed between the two representations of different viewpoints along the feature dimension:

$$\mathcal{Z} \triangleq \left(\widetilde{Z}'_p\right)^T \widetilde{Z}'_q \quad (10)$$

$\widetilde{Z}'(H \times D)$ is the representation obtained by normalizing Z' along the sample dimension.

\mathcal{L}_{VB} aims to push the diagonal elements of \mathcal{Z} towards 1, so that the representations are invariant to random geometric transformations. Meanwhile, by forcing the off-diagonal elements towards 0, we decorrelate different vector components of the representations, so that they contain non-redundant information about the original point cloud.

E. Pointly-supervised Scene Parsing

After self-supervised representation learning with the proposed viewpoint bottleneck loss \mathcal{L}_{VB} , we fine-tune on the pre-trained backbone by adding a scene parsing head (shown as light blue blocks in Fig.3) with $\{P_i, S_i\}$. This training scheme is much better than directly training with $\{P_i, S_i\}$, since the intrinsic structure between enormous unlabelled points are fully leveraged by self-supervised pre-training.

IV. EXPERIMENTS

A. Datasets

1) *Dataset for SSRL*: In this study, we use the official training split of ScanNet for unsupervised representation pre-training. ScanNet is a large-scale RGB-D video dataset with 3D mesh reconstructions of indoor scenes. It contains over 1500 scans reconstructed from around 2.5 million views. This dataset is annotated with both point-level and instance-level semantic labels. These labels are defined in a protocol of 20 categories. The official training split has 1201 scans.

2) *Dataset for pointly-supervised 3D scene parsing*: For fair comparison, we use the point annotations provided by [8] during fine-tuning. Four settings are evaluated, in which only 20 points, 50 points, 100 points, or 200 points of one point cloud in the training split have semantic labels. Other unlabeled points are ignored during the calculation of cross entropy loss Eq. 1. We firstly evaluate on the official validation set of 312 scans, using the mean intersection of union (mIOU) metric. We also provide quantitative results on the held-out test set, which is reported by an online server¹.

B. Implementation details

Then, we sample a combination of following transformations to apply to the selected point cloud:

- 1 Random rotation. We rotate the point cloud along z-axis by a random angle sampled from $\mathcal{U}[0, 2\pi]$.
- 2 Random mirroring. For each axis, we apply mirroring transformation with a probability of 0.5.
- 3 Random chromatic jitter. For each channel, we apply a noise sampled from $\mathcal{N}(0, 255 \times 0.05)$.

Our Sparse ConvUnet is implemented with the MinkowskiNet codebase [34], taking both 3D coordinates and point-wise RGB values as inputs. After farthest point sampling, a subset of 1024 points are selected as the abstraction of a point cloud. To investigate the robustness of VB, we inspect three settings for feature dimension D : 256, 512, and 1024.

For SSRL, all experiments are trained with a batch size 2 for 20000 iterations on two GeForce RTX 3090 GPUs, using a SGD optimizer with a momentum of 0.99 and an initial learning rate of 0.1. The learning rate is decayed according to a polynomial rule.

The pointly-supervised scene parsing experiments are trained with a batch size 12 for 30000 iterations on two GeForce RTX 3090 GPUs with the same optimizer setting. For both pre-training and fine-tuning experiments, the voxel size for Sparse ConvUNet is set to 2.0 cm.

C. Results and Analysis

1) *Results on ScanNet validation set*: Firstly, we show the effectiveness of viewpoint bottleneck on the ScanNet validation set. Quantitative results are summarized in Table.I. Baseline means training on point supervision without any SSRL. CSC stands for the contrastive scene context method [8], which is a contrastive learning scheme applied on local point cloud partitions. Our method is denoted as VB with

¹http://kaldir.vc.in.tum.de/scannet_benchmark/data_efficient/

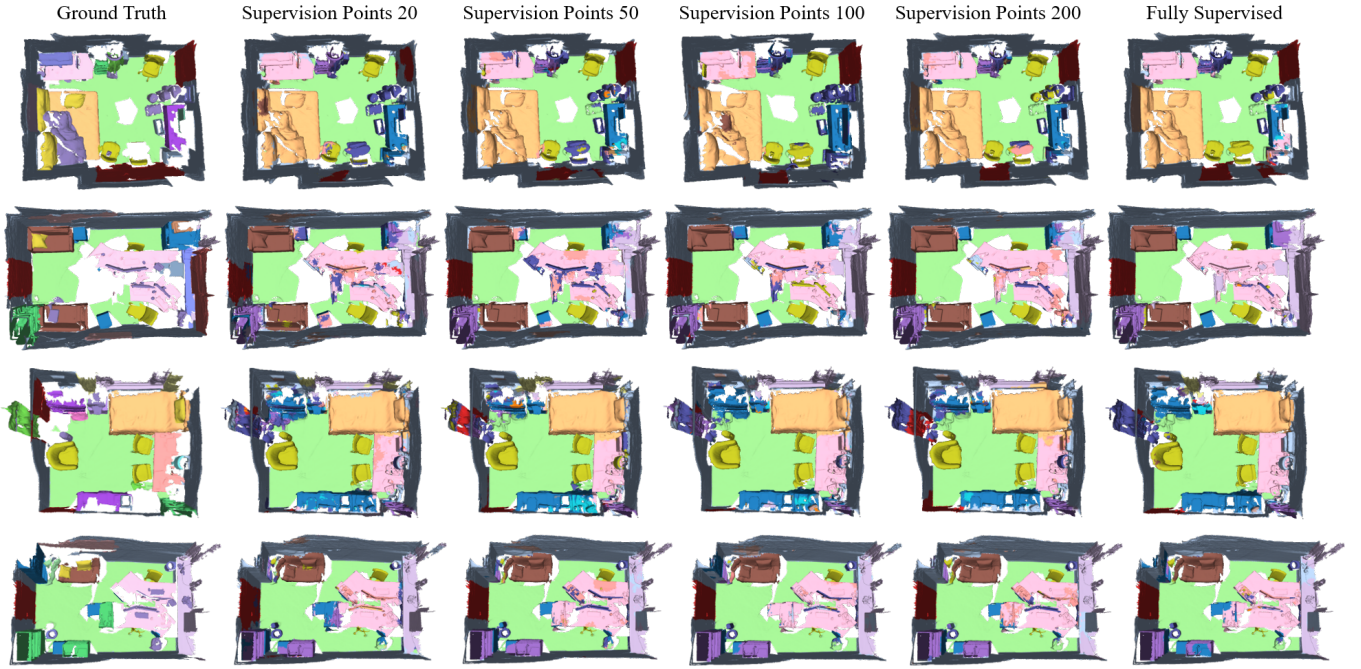


Fig. 6. Qualitative visualizations for point-supervised 3D scene parsing. The first column is ground truth and the last is generated by a fully-supervised model. The middle columns are generated by models pretrained by viewpoint bottleneck and supervised by sparse point annotations.

feature dimension D marked in brackets. For fair comparison, the network architectures are exactly the same.

Viewpoint bottleneck achieves clearly better results than CSC, in all four settings. In the 50 points setting, VB outperforms CSC by +3.2 mIOU. In the 20 and 100 points settings, the positive margins are also clear. In the 200 points setting, due to performance saturation, our quantitative results are comparable to CSC. Note that better performance in the down-stream pointily-supervised scene parsing task is not the only advantage of viewpoint bottleneck. As mentioned before, our method is easier to implement and tune than contrastive learning, as no sample pairs need to be selected.

Our method also out-performs the baseline by large margins. As shown in Table. I, in the 20 points setting, VB brings +11.1 mIOU over the trivial point supervision baseline. This demonstrates that viewpoint bottleneck is an effective solution for pointily-supervised 3D scene parsing, as rich representations that capture the intrinsic structure of point clouds are firstly learnt in an unsupervised manner. An interesting fact is that with the supervision point number decreases, the margins grow bigger, for both CSC and VB.

Qualitative results with different numbers of supervised points are shown in Fig.7. With the number of supervision points increasing, from 20 points to 200 points, the parsing results are getting closer to the fully-supervised setting. More qualitative results and category-wise quantitative results are provided in the supplementary material.

2) *Results on ScanNet test set:* We also evaluate on the held-out test set by submitting to an online server, with results shown in Table. II. Only comparable 3D SSRL methods are listed. Compared with CSC_LA_SEM [8] and

TABLE III
RESULTS ON SCANNET VALIDATION SET USING FULL SUPERVISION

	mIOU
Baseline	71.0
VB (1024)	71.9 (+0.9)

PointContrast_LA_SEM [7], We achieve better performance in three settings. In the 20 points setting, our results are roughly the same as [7]. There are other complicated method with iterative pseudo label generation like [36], which are not compared here due to the concern of fairness.

3) *Results with full supervision:* Although our goal is effective pointily-supervised scene parsing, we also evaluate with full supervision. As shown in Table.III, VB pre-training improves the fully supervised baseline by +0.9 mIOU.

V. CONCLUSION

In this paper, we address the challenging problem of learning 3D scene parsing models with only semantic annotations on sparse points. We develop a self-supervised representation learning framework named viewpoint bottleneck. We leverage a principled objective motivated by information theory and develops it into a practical surrogate loss. Pre-training with viewpoint bottleneck captures rich intrinsic structures between enormous unlabelled points. Pointily-supervised scene parsing performance on the public benchmark ScanNet is significantly improved, while reaching a new state-of-the-art among 3D SSRL methods.

REFERENCES

- [1] Newcombe, R.A., Izadi, S., Hilliges, O., Molyneaux, D., Kim, D., Davison, A.J., Kohi, P., Shotton, J., Hodges, S. and Fitzgibbon, A., 2011, October. Kinectfusion: Real-time dense surface mapping and tracking. In 2011 10th IEEE international symposium on mixed and augmented reality (pp. 127-136). IEEE.
- [2] Han, L. and Fang, L., 2018, June. FlashFusion: Real-time Globally Consistent Dense 3D Reconstruction using CPU Computing. In *Robotics: Science and Systems* (Vol. 1, No. 6, p. 7).
- [3] Dai, A., Chang, A.X., Savva, M., Halber, M., Funkhouser, T. and Nießner, M., 2017. Scannet: Richly-annotated 3d reconstructions of indoor scenes. In *Proceedings of the IEEE conference on computer vision and pattern recognition* (pp. 5828-5839).
- [4] Hinton, G.E. and Salakhutdinov, R.R., 2006. Reducing the dimensionality of data with neural networks. *science*, 313(5786), pp.504-507.
- [5] Doersch, C., Gupta, A. and Efros, A.A., 2015. Unsupervised visual representation learning by context prediction. In *Proceedings of the IEEE international conference on computer vision* (pp. 1422-1430).
- [6] He, K., Fan, H., Wu, Y., Xie, S. and Girshick, R., 2020. Momentum contrast for unsupervised visual representation learning. In *Proceedings of the IEEE/CVF Conference on Computer Vision and Pattern Recognition* (pp. 9729-9738).
- [7] Xie, S., Gu, J., Guo, D., Qi, C.R., Guibas, L. and Litany, O., 2020, August. Pointcontrast: Unsupervised pre-training for 3d point cloud understanding. In *European Conference on Computer Vision* (pp. 574-591). Springer, Cham.
- [8] Hou, J., Graham, B., Nießner, M. and Xie, S., 2021. Exploring data-efficient 3d scene understanding with contrastive scene contexts. In *Proceedings of the IEEE/CVF Conference on Computer Vision and Pattern Recognition* (pp. 15587-15597).
- [9] Liu, Y., Yi, L., Zhang, S., Fan, Q., Funkhouser, T. and Dong, H., 2020. P4Contrast: Contrastive Learning with Pairs of Point-Pixel Pairs for RGB-D Scene Understanding. *arXiv preprint arXiv:2012.13089*.
- [10] Zbontar, J., Jing, L., Misra, I., LeCun, Y. and Deny, S., 2021. Barlow twins: Self-supervised learning via redundancy reduction. *arXiv preprint arXiv:2103.03230*.
- [11] Bardes, A., Ponce, J. and LeCun, Y., 2021. Vicreg: Variance-invariance-covariance regularization for self-supervised learning. *arXiv preprint arXiv:2105.04906*.
- [12] Li, Y., Pogodin, R., Sutherland, D.J. and Gretton, A., 2021. Self-Supervised Learning with Kernel Dependence Maximization. *arXiv preprint arXiv:2106.08320*.
- [13] Liu, Y., Fan, Q., Zhang, S., Dong, H., Funkhouser, T. and Yi, L., 2021. Contrastive Multimodal Fusion with TupleInfoNCE. *arXiv preprint arXiv:2107.02575*.
- [14] Oord, A. V. D., Li, Y., and Vinyals, O., 2018. Representation learning with contrastive predictive coding. *arXiv preprint arXiv:1807.03748*.
- [15] Qian, R., Wei, Y., Shi, H., Li, J., Liu, J., and Huang, T., 2019. Weakly supervised scene parsing with point-based distance metric learning. In *Proceedings of the AAAI Conference on Artificial Intelligence* (Vol. 33, No. 01, pp. 8843-8850).
- [16] Dai, J., He, K., and Sun, J., 2015. Boxsup: Exploiting bounding boxes to supervise convolutional networks for semantic segmentation. In *Proceedings of the IEEE international conference on computer vision* (pp. 1635-1643).
- [17] Wei, Y., Liang, X., Chen, Y., Shen, X., Cheng, M. M., Feng, J., ... and Yan, S., 2016. Stc: A simple to complex framework for weakly-supervised semantic segmentation. *IEEE transactions on pattern analysis and machine intelligence*, 39(11), 2314-2320.
- [18] Ahn, J., and Kwak, S., 2018. Learning pixel-level semantic affinity with image-level supervision for weakly supervised semantic segmentation. In *Proceedings of the IEEE Conference on Computer Vision and Pattern Recognition* (pp. 4981-4990).
- [19] Wei, J., Lin, G., Yap, K. H., Hung, T. Y., and Xie, L., 2020. Multi-path region mining for weakly supervised 3d semantic segmentation on point clouds. In *Proceedings of the IEEE/CVF Conference on Computer Vision and Pattern Recognition* (pp. 4384-4393).
- [20] Wang, H., Rong, X., Yang, L., Feng, J., Xiao, J., and Tian, Y., 2020. Weakly supervised semantic segmentation in 3D graph-structured point clouds of wild scenes. *arXiv preprint arXiv:2004.12498*.
- [21] Pathak, D., Krahenbuhl, P., Donahue, J., Darrell, T., and Efros, A. A., 2016. Context encoders: Feature learning by inpainting. In *Proceedings of the IEEE conference on computer vision and pattern recognition* (pp. 2536-2544).
- [22] Zhang, R., Isola, P., and Efros, A. A., 2017. Split-brain autoencoders: Unsupervised learning by cross-channel prediction. In *Proceedings of the IEEE Conference on Computer Vision and Pattern Recognition* (pp. 1058-1067).
- [23] Doersch, C., Gupta, A., and Efros, A. A., 2015. Unsupervised visual representation learning by context prediction. In *Proceedings of the IEEE international conference on computer vision* (pp. 1422-1430).
- [24] Gidaris, S., Singh, P., and Komodakis, N., 2018. Unsupervised representation learning by predicting image rotations. *arXiv preprint arXiv:1803.07728*.
- [25] Zhao, H., Lu, M., Yao, A., Guo, Y., Chen, Y. and Zhang, L., 2020. Pointly-supervised scene parsing with uncertainty mixture. *Computer Vision and Image Understanding*, 200, p.103040.
- [26] Chen, T., Kornblith, S., Norouzi, M., and Hinton, G., 2020. A simple framework for contrastive learning of visual representations. In *International conference on machine learning* (pp. 1597-1607). PMLR.
- [27] Chopra, S., Hadsell, R., and LeCun, Y., 2005. Learning a similarity metric discriminatively, with application to face verification. In 2005 IEEE Computer Society Conference on Computer Vision and Pattern Recognition (CVPR'05) (Vol. 1, pp. 539-546). IEEE.
- [28] Grill, J. B., Strub, F., Althé, F., Tallec, C., Richemond, P. H., Buchatskaya, E., ... and Valko, M., 2020. Bootstrap your own latent: A new approach to self-supervised learning. *arXiv preprint arXiv:2006.07733*.
- [29] Chen, X., and He, K. 2021. Exploring simple siamese representation learning. In *Proceedings of the IEEE/CVF Conference on Computer Vision and Pattern Recognition* (pp. 15750-15758).
- [30] Tishby, N., and Zaslavsky, N., 2015. Deep learning and the information bottleneck principle. In 2015 IEEE Information Theory Workshop (ITW) (pp. 1-5). IEEE.
- [31] Tishby, N., Pereira, F. C., and Bialek, W., 2000. The information bottleneck method. *arXiv preprint physics/0004057*.
- [32] Cover, T. M., 1999. *Elements of information theory*. John Wiley & Sons (pp. 254-256).
- [33] Cai, T. T., Liang, T., and Zhou, H. H., 2015. Law of log determinant of sample covariance matrix and optimal estimation of differential entropy for high-dimensional Gaussian distributions. *Journal of Multivariate Analysis*, 137, 161-172.
- [34] Choy, C., Gwak, J., and Savarese, S., 2019. 4d spatio-temporal convnets: Minkowski convolutional neural networks. In *Proceedings of the IEEE/CVF Conference on Computer Vision and Pattern Recognition* (pp. 3075-3084).
- [35] Huang, S., Xie, Y., Zhu, S.C. and Zhu, Y., 2021. Spatio-temporal Self-Supervised Representation Learning for 3D Point Clouds. *arXiv preprint arXiv:2109.00179*.
- [36] Liu, Z., Qi, X. and Fu, C.W., 2021. One Thing One Click: A Self-Training Approach for Weakly Supervised 3D Semantic Segmentation. In *Proceedings of the IEEE/CVF Conference on Computer Vision and Pattern Recognition* (pp. 1726-1736).

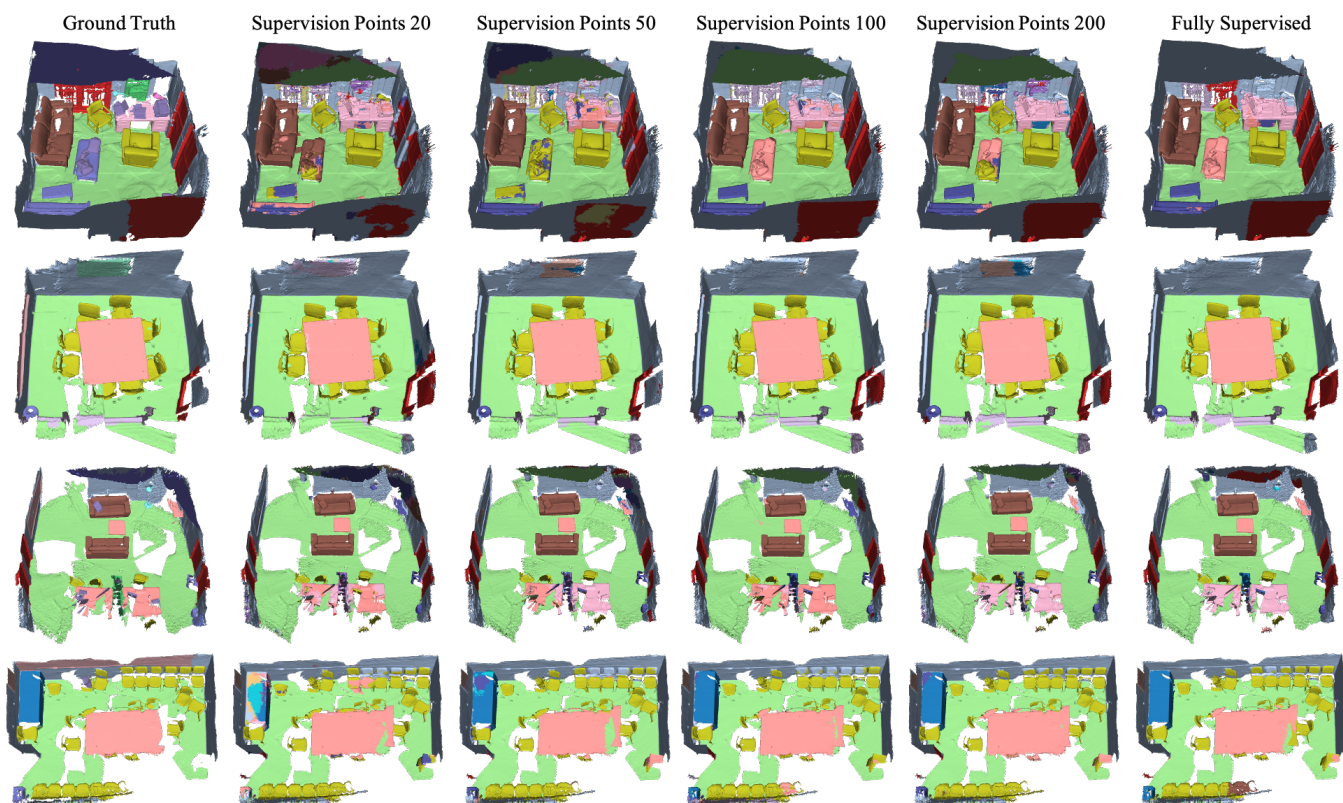


Fig. 7. More qualitative results.

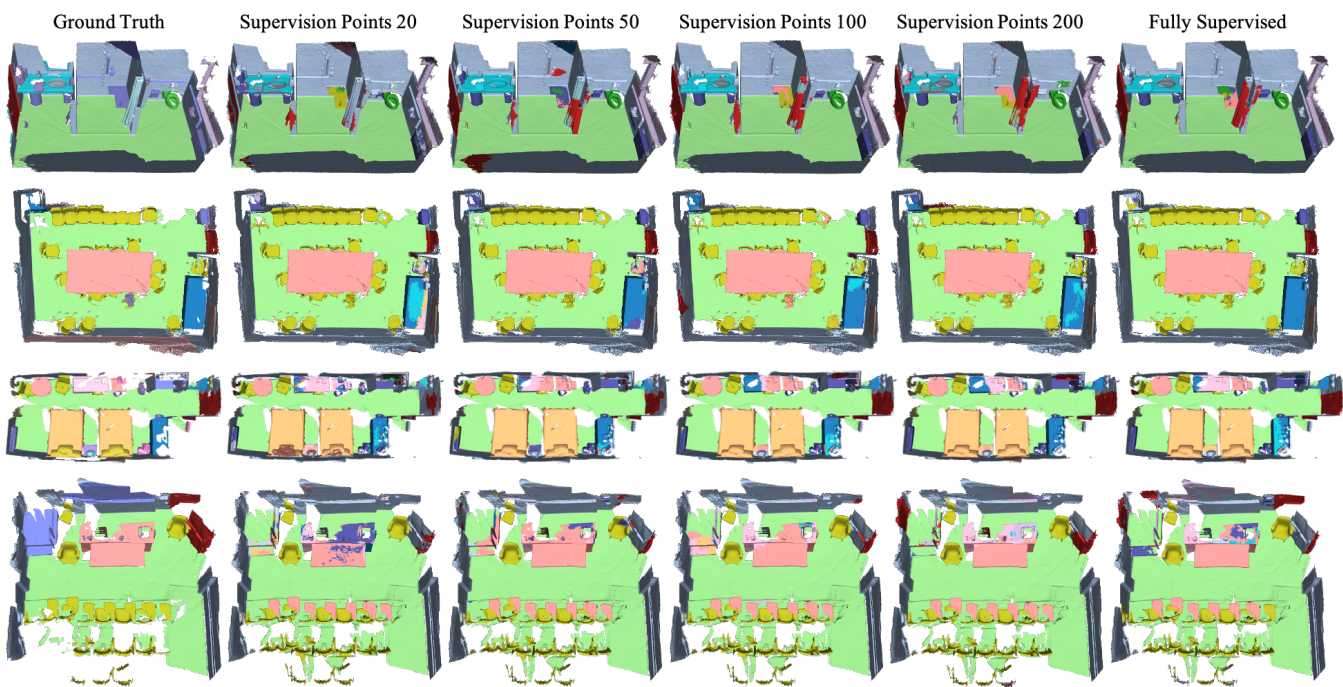


Fig. 7. More qualitative results (cont.).

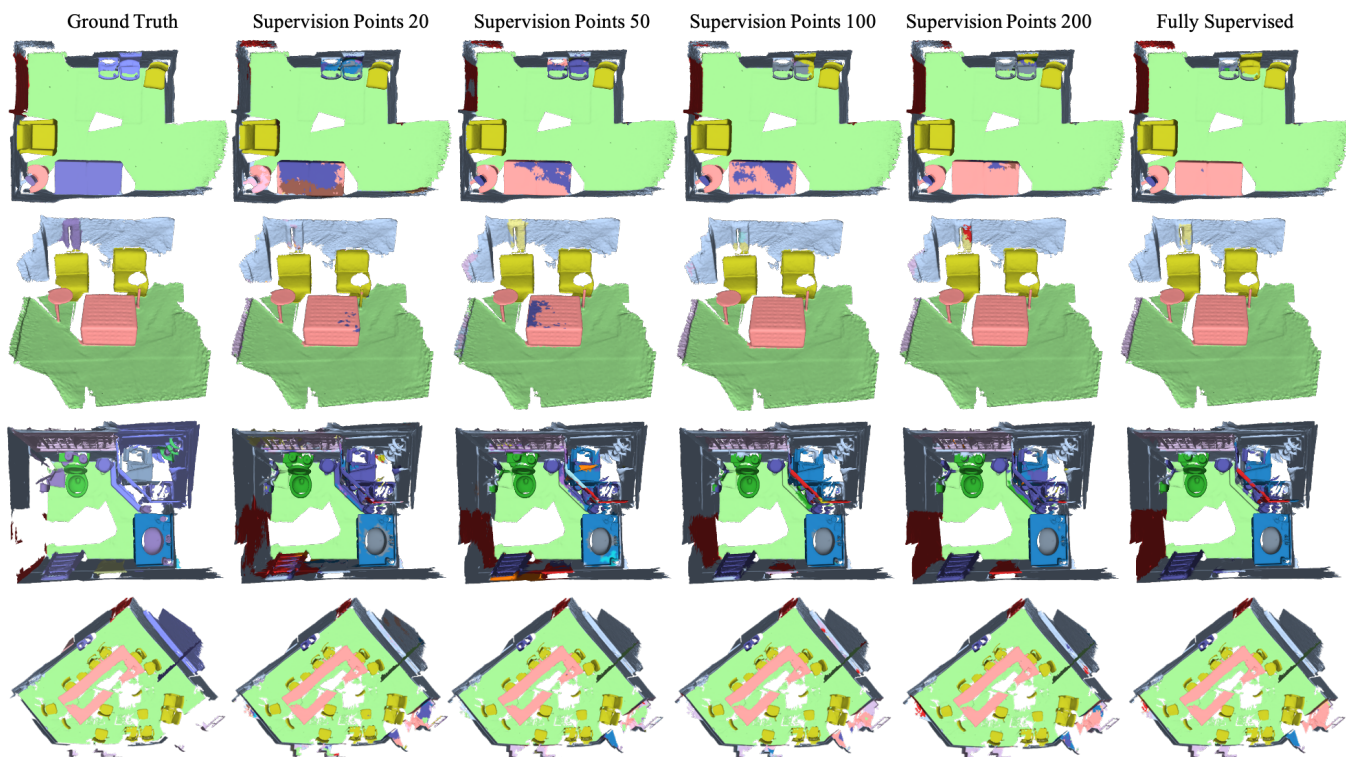


Fig. 7. More qualitative results (cont.).

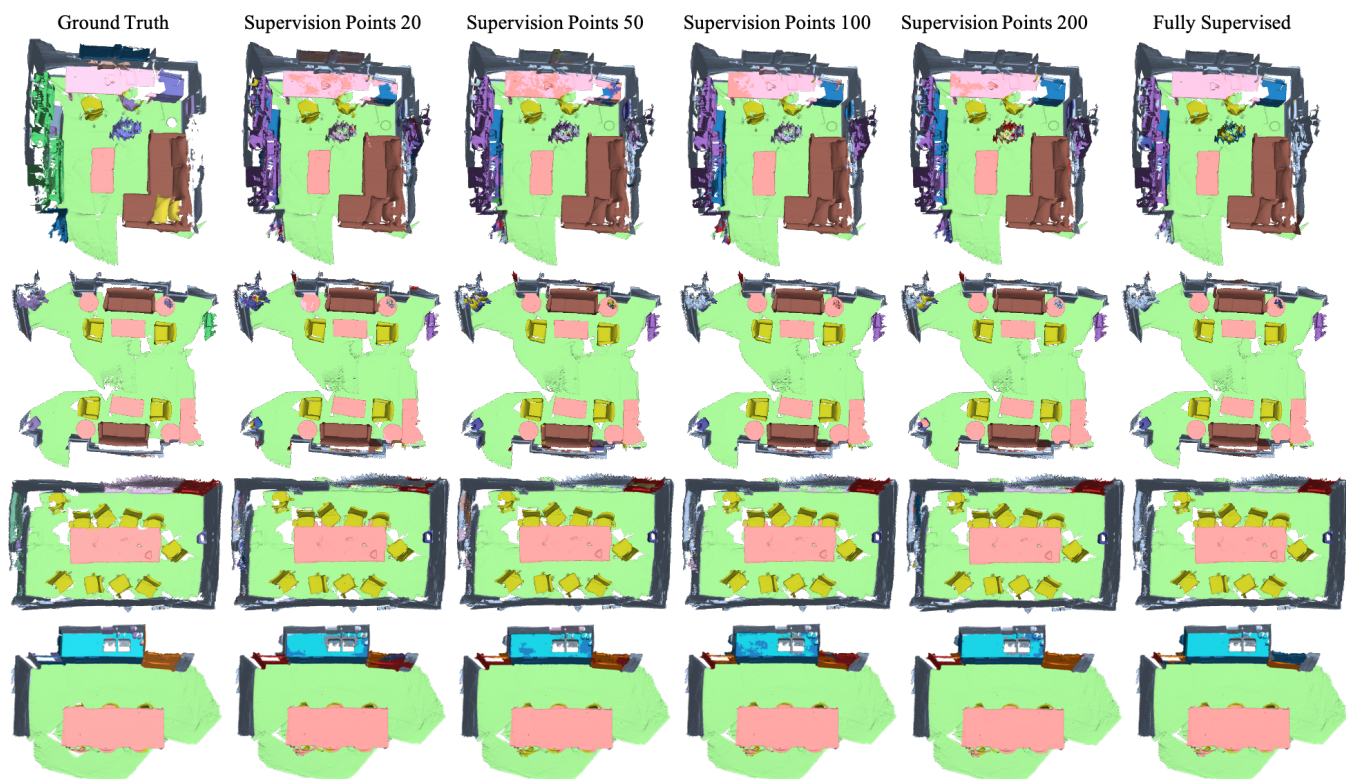


Fig. 7. More qualitative results (cont.).

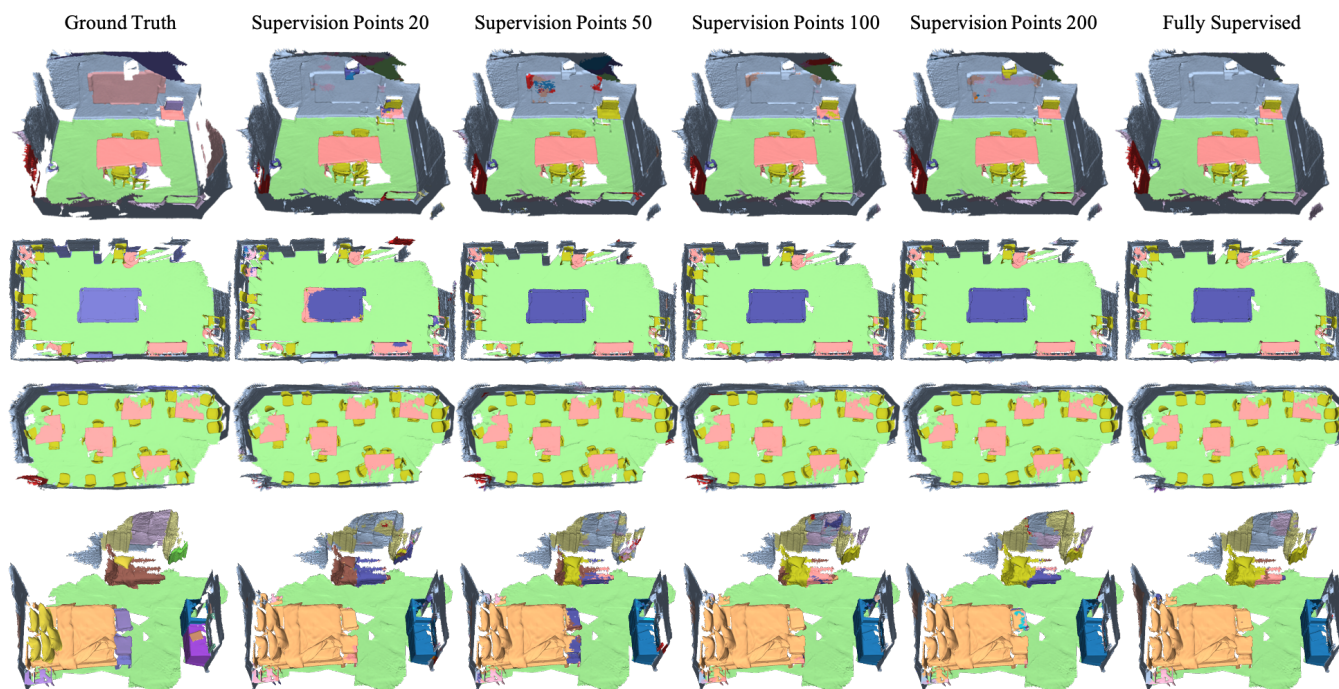


Fig. 7. More qualitative results (cont.).

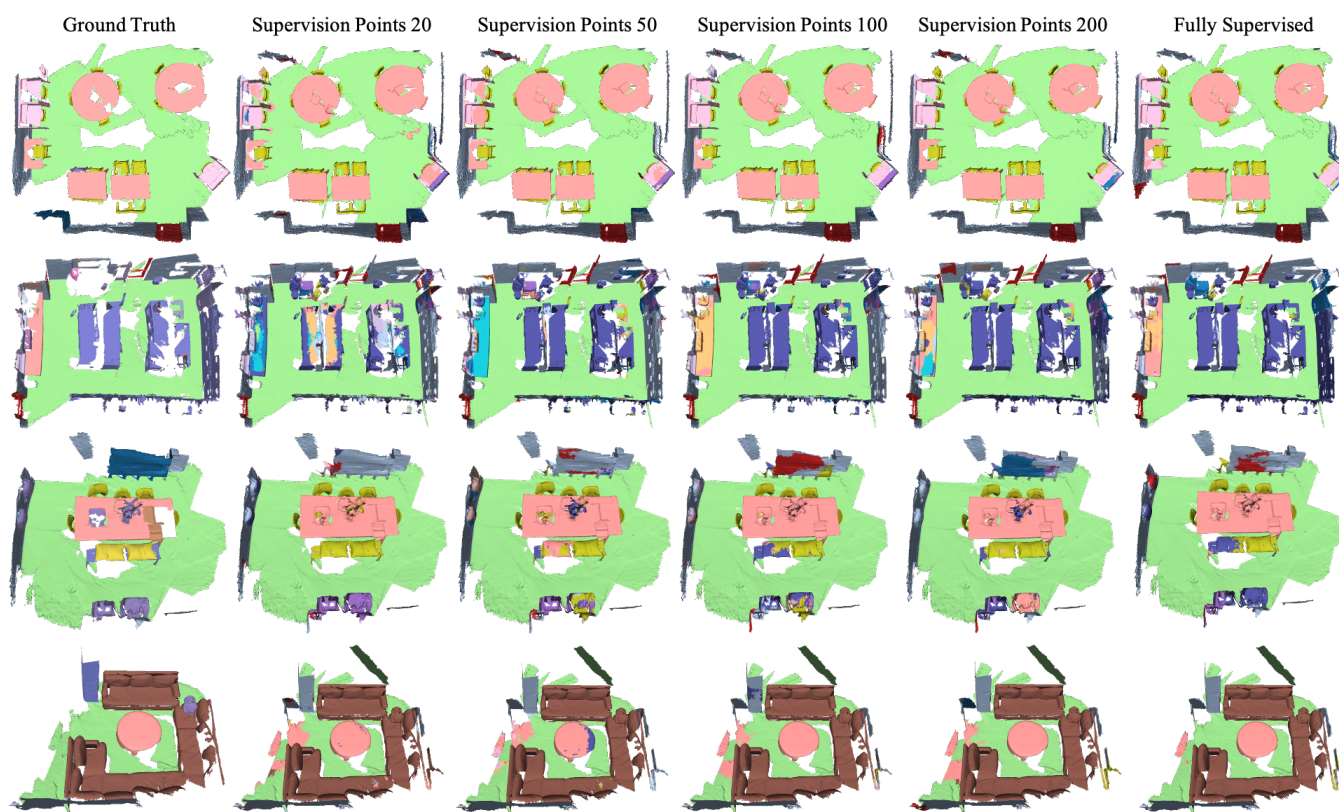


Fig. 7. More qualitative results (cont.).

TABLE IV
SCANNet 3D SEMANTIC LABEL WITH LIMITED ANNOTATIONS BENCHMARK (mIOU:%)

200 points	bathtub	bed	bookshelf	cabinet	chair	counter	curtain	desk	door	floor	AVG IOU
Viewpoint_BN.LA.AIR(ours)	84.7	73.2	72.4	61.3	82.7	44.3	74.2	56.2	55.1	94.7	66.9
CSC.LA.SEM	85.7	75.6	76.3	64.7	85.2	43.2	68.4	54.3	51.4	94.8	66.5
PointContrast.LA.SEM	71.7	77.5	75.4	62.6	80.4	39.1	68.9	48.5	57.2	94.5	65.3
200 points	O.F.	picture	refrigerator	S.C.	sink	sofa	table	toilet	wall	window	
Viewpoint_BN.LA.AIR(ours)	44.1	21.8	65.0	75.3	62.1	76.5	60.1	90.5	81.4	61.8	
CSC.LA.SEM	46.9	17.9	59.9	70.2	62.0	78.9	61.4	91.1	81.5	60.7	
PointContrast.LA.SEM	44.8	23.2	60.3	81.3	59.1	77.5	53.7	88.5	81.6	60.8	
100 points	bathtub	bed	bookshelf	cabinet	chair	counter	curtain	desk	door	floor	AVG IOU
Viewpoint_BN.LA.AIR(ours)	77.8	73.1	68.8	61.7	81.2	44.6	73.9	61.8	54.0	94.5	65.0
CSC.LA.SEM	76.1	70.7	70.3	64.2	81.3	43.6	65.9	50.2	51.6	94.5	64.4
PointContrast.LA.SEM	69.4	73.8	73.1	65.3	81.7	46.7	65.1	51.7	52.2	94.6	63.6
100 points	O.F.	picture	refrigerator	S.C.	sink	sofa	table	toilet	wall	window	
Viewpoint_BN.LA.AIR(ours)	41.5	20.4	62.3	67.6	59.4	74.4	57.6	86.8	81.1	58.2	
CSC.LA.SEM	48.7	23.8	53.8	67.8	65.9	73.9	56.8	91.5	81.1	56.6	
PointContrast.LA.SEM	47.9	19.8	57.5	52.6	64.9	74.7	56.9	84.5	80.3	60.0	
50 points	bathtub	bed	bookshelf	cabinet	chair	counter	curtain	desk	door	floor	AVG IOU
Viewpoint_BN.LA.AIR(ours)	81.2	74.3	65.4	57.9	80.0	46.2	71.3	53.3	51.6	94.4	62.3
CSC.LA.SEM	74.7	73.1	67.9	60.3	81.5	40.0	64.8	45.3	48.1	94.4	61.2
PointContrast.LA.SEM	84.4	73.1	68.1	59.0	79.1	34.8	68.9	50.3	50.2	94.2	61.4
50 points	O.F.	picture	refrigerator	S.C.	sink	sofa	table	toilet	wall	window	
Viewpoint_BN.LA.AIR(ours)	43.4	21.5	43.7	52.1	60.1	72.0	56.3	88.4	80.0	53.4	
CSC.LA.SEM	42.1	17.3	50.7	62.3	58.8	69.0	54.5	87.7	77.8	54.1	
PointContrast.LA.SEM	36.1	15.4	48.4	62.4	59.1	70.8	52.4	87.4	79.3	53.6	
20 points	bathtub	bed	bookshelf	cabinet	chair	counter	curtain	desk	door	floor	AVG IOU
Viewpoint_BN.LA.AIR(ours)	74.7	57.4	63.1	45.6	76.2	35.5	63.9	41.2	40.4	94.0	54.8
CSC.LA.SEM	65.9	63.8	57.8	41.7	77.5	25.4	53.7	39.6	43.9	93.9	53.1
PointContrast.LA.SEM	73.5	67.6	60.1	47.5	79.4	28.8	62.1	37.8	43.0	94.0	55.0
20 points	O.F.	picture	refrigerator	S.C.	sink	sofa	table	toilet	wall	window	
Viewpoint_BN.LA.AIR(ours)	33.5	10.7	27.7	64.5	49.5	66.6	51.7	81.8	74.0	43.1	
CSC.LA.SEM	28.4	8.3	41.1	59.9	48.8	69.8	44.4	78.5	74.7	44.0	
PointContrast.LA.SEM	30.3	8.9	37.9	58.0	53.1	68.9	42.2	85.2	75.8	46.8	

* The O.F. is the other furniture and the S.C. is the shower curtain.

TABLE V
POINTLY-SUPERVISED 3D PARSING RESULTS ON THE SCANNET VALIDATION SET (mIOU:%)

200 points	wall	floor	cabinet	bed	chair	sofa	table	door	window	bookshelf	AVG IOU
VB (256)	82.3	95.6	60.8	78.6	88.8	82.2	72.4	59.6	52.9	76.1	68.4
VB (512)	82.8	95.6	61.3	81.6	89.0	84.6	70.0	59.1	55.0	75.2	68.5
VB (1024)	82.6	95.5	60.8	80.6	89.2	83.6	70.9	57.8	53.6	76.3	68.4
200 points	picture	counter	desk	curtain	refrigerator	S.C.	toilet	sink	bathtub	O.F.	
VB (256)	27.5	59.2	60.8	68.3	48.3	66.9	87.8	63.4	86.6	49.2	
VB (512)	27.1	59.5	58.5	69.3	44.2	63.1	89.9	63.6	85.6	55.0	
VB (1024)	29.9	60.1	59.4	68.6	49.1	61.9	89.7	61.7	87.1	49.8	
100 points	wall	floor	cabinet	bed	chair	sofa	table	door	window	bookshelf	AVG IOU
VB (256)	81.1	95.4	59.2	78.6	88.2	82.9	67.7	56.2	51.9	71.9	66.5
VB (512)	81.2	95.6	57.9	76.4	88.8	83.9	70.9	56.4	53.2	72.6	66.8
VB (1024)	81.0	95.5	58.6	77.7	88.7	82.6	70.2	54.5	51.0	74.0	66.5
100 points	picture	counter	desk	curtain	refrigerator	S.C.	toilet	sink	bathtub	O.F.	
VB (256)	23.9	55.1	55.0	65.4	50.8	64.0	89.7	57.9	85.5	48.6	
VB (512)	23.4	56.9	56.1	67.2	46.7	64.5	90.3	62.6	85.0	47.0	
VB (1024)	24.9	55.9	56.5	65.3	47.1	59.2	92.6	60.5	85.1	48.6	
50 points	wall	floor	cabinet	bed	chair	sofa	table	door	window	bookshelf	AVG IOU
VB (256)	79.4	95.3	55.7	77.7	86.8	79.2	67.5	50.2	47.5	72.7	63.3
VB (512)	79.8	95.2	56.0	76.1	87.1	80.7	66.3	52.2	48.5	71.3	63.6
VB (1024)	79.5	95.1	56.3	77.7	87.1	81.7	66.9	50.8	47.2	72.4	63.7
50 points	picture	counter	desk	curtain	refrigerator	S.C.	toilet	sink	bathtub	O.F.	
VB (256)	19.3	54.3	52.7	63.2	39.4	58.3	83.2	57.1	83.0	44.1	
VB (512)	18.6	52.1	51.3	63.5	42.9	60.2	86.4	55.7	82.6	46.2	
VB (1024)	15.5	51.1	52.0	62.7	40.3	62.5	89.2	56.2	84.1	44.8	
20 points	wall	floor	cabinet	bed	chair	sofa	table	door	window	bookshelf	AVG IOU
VB (256)	74.6	94.9	46.6	67.3	83.7	75.9	59.9	38.8	38.8	66.9	56.2
VB (512)	74.6	95.0	49.0	71.1	85.5	78.7	63.6	39.3	37.0	66.7	57.0
VB (1024)	74.8	94.8	48.3	70.4	84.6	76.1	62.1	37.7	38.9	67.2	56.3
20 points	picture	counter	desk	curtain	refrigerator	S.C.	toilet	sink	bathtub	O.F.	
VB (256)	14.3	45.6	44.1	55.9	30.7	52.5	76.3	46.0	78.1	33.8	
VB (512)	10.9	45.3	48.7	55.7	29.0	51.2	81.0	48.8	73.7	35.2	
VB (1024)	11.5	43.9	43.5	54.0	30.1	46.0	78.8	48.2	78.6	36.3	

* The O.F. is the other furniture and the S.C. is the shower curtain.

TABLE VI
RESULTS ON SCANNET VALIDATION SET USING FULL SUPERVISION (mIOU:%)

Full Supervision	wall	floor	cabinet	bed	chair	sofa	table	door	window	bookshelf	AVG IOU
Baseline	84.9	96.0	63.1	81.6	90.1	83.6	73.1	62.8	59.1	80.0	71.0
VB (1024)	95.2	96.0	65.8	79.9	90.5	83.2	73.3	64.8	60.3	80.7	71.9
Full Supervision	picture	counter	desk	curtain	refrigerator	S.C.	toilet	sink	bathtub	O.F.	
Baseline	31.9	65.1	61.0	75.7	51.1	66.4	91.9	63.6	85.9	52.6	
VB (1024)	31.8	66.1	62.8	74.3	56.0	64.5	92.7	67.7	83.4	59.8	

* The O.F. is the other furniture and the S.C. is the shower curtain.